RSC Advances

PAPER

View Article Online
View Journal | View Issue

Cite this: *RSC Adv.*, 2018, **8**, 37618

Enhanced upconversion fluorescent probe of single $NaYF_4$:Yb^{3+}/Er^{3+}/Zn^{2+} nanoparticles for copper ion detection†

Baobao Zhang, Jiajia Meng, Xiaohu Mi, Changjian Zhang, Zhenglong Zhang* and Hairong Zheng*

Received 25th August 2018
Accepted 31st October 2018

DOI: 10.1039/c8ra07103a

rsc.li/rsc-advances

Surface modified $NaYF_4$:Yb^{3+}/Er^{3+}/Zn^{2+} upconversion nanoparticles were obtained by using branched polyethylenimine (PEI). Strong fluorescence emission was observed and the influence of copper ions on the fluorescence emission of the PEI-modified $NaYF_4$:Yb^{3+}/Er^{3+}/Zn^{2+} nanoparticles was investigated. It was found that the fluorescence emission can be quenched through luminescence resonance energy transfer from the particle to the copper ions. The results show that the PEI modified $NaYF_4$:Yb^{3+}/Er^{3+}/Zn^{2+} nanoparticle can be used as a fluorescent probe for highly sensitive and selective detection of copper ions.

1. Introduction

Rare-earth doped up-conversion nanoparticles (UCNPs) have attracted much attention since 1990s with their excellent upconversion luminescence properties such as large anti-Stokes shift, luminescence with rich color, narrowband emission and good optical stability.[1–6] Up to now lots of research on the basic issues of synthesis and luminescence properties of UCNPs has been carried out.[7–11] Meanwhile, the application of UCNPs in bioimaging and detection, photothermal therapy, contaminant detection, solar cells, anti-counterfeiting technology, three-dimensional displays and so on have been conducted.[12–16] In the development of its application, the detection of heavy metal ions by fluorescent UCNP probes has become a very promising subject due to its advantages such as convenient operation, low cost, highly sensitive and selective.[17–19] Considering the important role of copper ion in biological systems and their widespread distribution, the development of fluorescent probe for highly sensitive detection of copper ion is of great significance for environmental protection and life science research.

Currently, most methods for detecting heavy metal ions by fluorescent probes are based on liquid phase. With this method, the sample is easy to prepare, but it needs to consume much more fluorescent probe material during the detection process, and the fluorescence emission intensity is easy to fluctuate significantly due to the possible uneven distribution of the fluorescent probes in the solution. While the strategy with single particle probe can avoid these problems and can further improve detection sensitivity.[20] However, compared with the powder samples of upconversion nanoparticles, the luminescence intensity of the single nanoparticle is usually very weak, which results in the difficulty of the single nanoparticle fluorescent probe for metal ion detection. In order to improve the luminescence intensity and detecting efficiency, researchers have proposed a variety of methods, such as ions co-doping, the introduction of transition metal ions, core–shell coating, plasmon resonance enhancement and so on.[21–25] Many studies have been reported on the introduction of smaller radius ions (Li^+, Mn^{2+}, Mg^{2+}, *etc.*)[26–28] in UCNPs to enhance the upconversion emission, but few studies on the introduction of Zn^{2+} ions into the rare-earth doped hexagonal phase $NaYF_4$ nanoparticles are presented.[29]

In this paper, $NaYF_4$:Yb^{3+}(20%)/Er^{3+}(2%)/Zn^{2+}(7%) nanoparticles with enhanced luminescence were successfully obtained by introducing Zn^{2+} ions in the hydrothermal synthesis process to the UCNPs. A method for high-sensitivity detection of copper ion by single $NaYF_4$:Yb^{3+}/Er^{3+}/Zn^{2+} nanoparticle fluorescent probe has been developed and reported. The linear detection range and the limit of single nanoparticle fluorescent probe for the copper ion detection were studied experimentally.

2. Experimental

2.1 Materials

$Er(NO_3)_3 \cdot 5H_2O$ (99.9%), $Yb(NO_3)_3 \cdot 5H_2O$ (99.9%), PEI (99.0%) and $Y(NO_3)_3 \cdot 6H_2O$ (99.8%) were purchased from Sigma Aldrich. $Zn(NO_3)_2 \cdot 6H_2O$ (99.0%), $CuCl_2 \cdot 2H_2O$ (99.0%), $NaNO_3$ (99.0%), NaF (98.0%), C_2H_5OH (99.7%), $C_6H_5Na_3O_7 \cdot 2H_2O$ (99.0%), $FeCl_3$ (97%), $SnCl_2 \cdot 2H_2O$ (98%), KCl (99.5%), $MgCl_2 \cdot 6H_2O$ (98%), NaCl (99.5%), NH_4Cl (99.5%) were purchased from Sinopharm Chemical Reagent Co., Ltd. (China).

School of Physics and Information Technology, Shaanxi Normal University, Xi'an 710119, P. R. China. E-mail: hrzheng@snnu.edu.cn; zlzhang@snnu.edu.cn

† Electronic supplementary information (ESI) available. See DOI: 10.1039/c8ra07103a

All the chemicals were used without further purification.

2.2 Characterization

Morphologies of $NaYF_4$:Yb^{3+}/Er^{3+} and $NaYF_4$:Yb^{3+}/Er^{3+}/Zn^{2+} particles were characterized by scanning electron microscope (SEM, FEI-Nova-450) and transmission electron microscopy (TEM, FEI-Tecnai G2 F20). Crystalline phase of the particle was studied by the powder X-ray diffraction (XRD, D8 Advance). The PEI modified $NaYF_4$:Yb^{3+}/Er^{3+}/Zn^{2+} nanoparticles were examined by Fourier transform infrared spectra (FTIR, TENSOR II). These samples were excited by a femtosecond laser at 980 nm with power of 100 mW (Coherent Mira 900-F). The spectral data and microscopic images were collected by the micro-spectroscopy system which consists of a spectrometer (Princeton Instruments SP2750i) equipped with charge coupled device (CCD, ACTON PIXIS 100) and microscopy (OLYMPUS BX51) equipped with camera (Thorlabs 4070C-USB).

2.3 Sample characterization

In order to obtain UCNPs with high luminescence efficiency and high surface to volume ratio so that a suitable single nanoparticle fluorescent probe can be designed,[30–32] the hexagonal $NaYF_4$:Yb^{3+}/Er^{3+} microdisks and $NaYF_4$:Yb^{3+}/Er^{3+}/Zn^{2+} nanoparticles were synthesized by hydrothermal method.[33] As shown by scanning electron microscope (SEM) images (Fig. 1(a and b)) and size distribution graphs (Fig. S1(a and b)†), the morphologies of particles are uniform hexagonal disks. According to X-ray diffraction (XRD) shown in Fig. S2,† the crystallization of particles matches to the hexagonal phase crystal. Comparing with $NaYF_4$:Yb^{3+}/Er^{3+} microdisks, we found that the diffraction peak position and intensity of the $NaYF_4$:Yb^{3+}/Er^{3+}/Zn^{2+} nanoparticles did not change significantly, which indicates the low content of Zn^{2+} ions in nanoparticles and less significant change of the crystal structure. Fig. 1(c and d) are typical morphology of the $NaYF_4$:Yb^{3+}/Er^{3+}/Zn^{2+} nanoparticle, which was further provided by TEM and HR-TEM. The spatial distribution of the Na, Y, F, Yb, Er, and Zn in the nanoparticle are shown by elemental mapping images (Fig. 1(e)) of the single $NaYF_4$:Yb^{3+}/Er^{3+}/Zn^{2+} nanoparticle, directly indicating that Zn^{2+} icons have been successfully incorporated into the nanoparticle.

3. Results and discussion

3.1 Property of luminescence emission

To study the effect of doped zinc ions on the emission property of the single UCNP, the luminescence emission spectra from single $NaYF_4$:Yb^{3+}/Er^{3+}/Zn^{2+} nanoparticle and single $NaYF_4$:Yb^{3+}/Er^{3+} microdisk were measured under the 980 nm laser excitation, which are shown in Fig. 2(a). Five dominant emission peaks at around 468 nm, 503 nm, 521 nm, 556 nm and 654 nm are displayed by both particles, which correspond to transitions of $^4G_{7/2} \rightarrow {}^4I_{13/2}$, $^4G_{11/2} \rightarrow {}^4I_{13/2}$, $^2H_{11/2} \rightarrow {}^4I_{15/2}$, $^4S_{3/2} \rightarrow {}^4I_{15/2}$ and $^4F_{9/2} \rightarrow {}^4I_{15/2}$, respectively. In the obtained emission spectra, the red emission intensity was similar for both particle of $NaYF_4$:Yb^{3+}/Er^{3+} and $NaYF_4$:Yb^{3+}/Er^{3+}/Zn^{2+} nanoparticle, while the green and blue light emission were enhanced for $NaYF_4$:Yb^{3+}/Er^{3+}/Zn^{2+} nanoparticle comparing with that from $NaYF_4$:Yb^{3+}/Er^{3+} microdisk. Taking into account the difference in the size of $NaYF_4$:Yb^{3+}/Er^{3+}/Zn^{2+} nanoparticle and $NaYF_4$:Yb^{3+}/Er^{3+} microdisk, the enhancement factors for blue, green, and red light emission per unit volume of the particle were 176, 45, and 20, respectively. Although such an estimation ignored the influence of absorption difference of particles and covered area of the excitation light spot *etc.*, the enhancement factor 10^1 to 10^2 was sufficient to show that the effect of Zn^{2+} ions to the enhancement of upconversion luminescence from the rare-earth doped single $NaYF_4$ particle was very significant. Our study on the enhancement mechanism and related reports suggest that the observed enhancement could be due to the

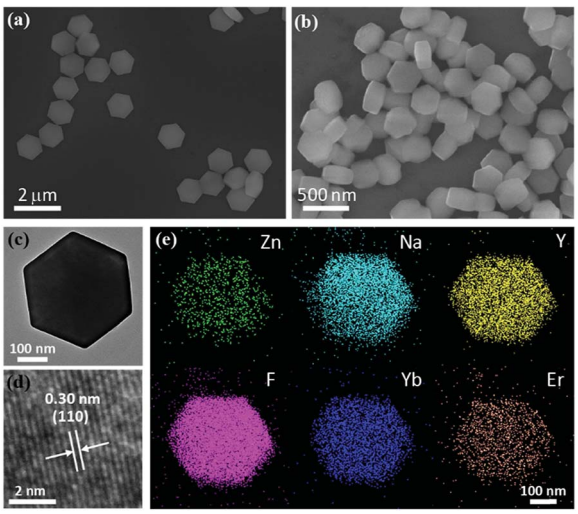

Fig. 1 (a) The SEM image of the $NaYF_4$:Yb^{3+}/Er^{3+} microdisks, (b)–(d) the SEM, TEM and HR-TEM images of the $NaYF_4$:Yb^{3+}/Er^{3+}/Zn^{2+} nanoparticles, (e) elemental mapping images of the $NaYF_4$:Yb^{3+}/Er^{3+}/Zn^{2+} nanoparticle.

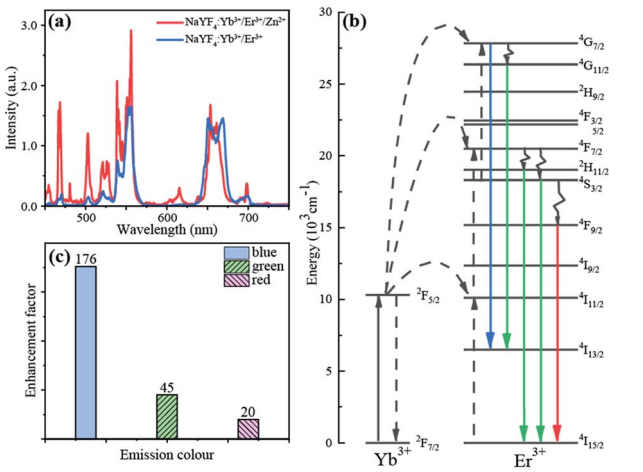

Fig. 2 (a) Luminescence spectra from single $NaYF_4$:Yb^{3+}/Er^{3+}/Zn^{2+} and $NaYF_4$:Yb^{3+}/Er^{3+} particle, (b) energy level diagram and possible transitions of Yb^{3+} and Er^{3+} ions, (c) enhancement factors for blue, green, and red light emission per unit volume of single particle.

local symmetry decrease of the crystal field around Er^{3+} ion by the introduction of Zn^{2+} ions into the particle.[29,34,35]

3.2 Fluorescent probe of single UCNP for Cu^{2+} detection

Since UCNP doped with zinc ions has much stronger luminescence emission and larger surface-to-volume ratio, we choose PEI-modified $NaYF_4$:Yb^{3+}/Er^{3+}/Zn^{2+} as single-particle fluorescent probe. In order to investigate the detection ability and detection limit of the particle probe for detecting Cu^{2+} ions, we designed the single particle detecting system that is shown by Fig. 3. The luminescence of PEI-modified $NaYF_4$:Yb^{3+}/Er^{3+}/Zn^{2+} nanoparticle might be quenched by copper ions and the concentration of copper ions can be calculated based on the degree of luminescence quenching.

In order to conduct the selective detection of copper ions, we modified the surface of the UCNPs with PEI by physical adsorption. As shown in Fig. 4(a), the PEI and PEI-modified UCNPs both exhibited characteristic absorption peak at 1648 cm^{-1} that was assigned to the bending vibration of NH_2 bond, since the absorption peak did not be observed from the unmodified UCNPs, this result indicates that PEI has been successfully modified on the particle for PEI-modified UCNPs. To examine the application possibility of PEI-modified UCNPs and the selection on the ions in the solution, the elemental distribution was characterized after adding 10 μL $CuCl_2$ solution that contains both Cu^{2+} and Cl^- ions to PEI-modified nanoparticle. Fig. 4(b) shows that a large amount of Cu^{2+} ions were adsorbed on the nanoparticle while chloride ions were seldomly detected. This indicates that the amino group contained in PEI can selectively bind with Cu^{2+} ions forming a complex with copper ions. Therefore, the modified nanoparticle can be a good candidate of single-particle fluorescent probe.

To illustrate the application of single PEI modified UCNP for detecting copper ions in solution, we conducted the experimental measurement with following procedure. First, the luminescence intensity of single-particle fluorescent probe was measured and the corresponding image was taken too. After that, 10 μL solution of 20 nM copper ions was completely added to the particle dropwise *in situ*, luminescence spectrum and microscopic image were recorded accordingly. Fig. 4(c) shows the luminescence spectra and corresponding images of the single particle probe before and after the addition of copper ion solution drop by drop. Obviously, after the copper ion solution was added, the luminescence intensity of the particle probe was significantly reduced. By integrating the luminescence intensity of the emission in the green region, we found that the degree of fluorescence quenching caused by copper ion solution was 52%, 77%, 93%, respectively. The degree of fluorescence quenching is estimated based on the formula of

$$Q_f = \frac{\int_{\lambda_1}^{\lambda_2} I_0(\lambda)d\lambda - \int_{\lambda_1}^{\lambda_2} I(\lambda)d\lambda}{\int_{\lambda_1}^{\lambda_2} I_0(\lambda)d\lambda} \times 100\%$$

where Q_f is the degree of fluorescence quenching after adding copper ion solution to the single particle probe. $I_0(\lambda)$ and $I(\lambda)$ are the luminescence intensity of the fluorescent probe at wavelength λ with and without the addition of the Cu^{2+} solution. Base on the previous investigation,[17] the resonance energy transfer from the Yb^{3+} ions in the excited state to copper ammine complexes might be the reason for fluorescence quenching of $NaYF_4$:Yb^{3+}/Er^{3+}/Zn^{2+} particle by Cu^{2+} ions.

To examine the influence of water solvent on the luminescence particle probe, we also carried out the spectral measurement of the probe particle by adding pure water solvent to it. It was found that the luminescence intensity of the single-particle fluorescent probe was also quenched obviously after water solvent added (see Fig. S4†). But the degree of luminescence quenching caused by water solvent was much less than that caused by copper ions. It was also found that the luminescence intensity of the bare $NaYF_4$:Yb^{3+}/Er^{3+}/Zn^{2+} particle (unmodified with PEI) did not present obvious change after adding copper ion solution or water solvent to it. Therefore, it is reasonable to use PEI modified single $NaYF_4$:Yb^{3+}/Er^{3+}/Zn^{2+} particle as a fluorescent probe for Cu^{2+} ion detection.

3.3 Sensitivity and selectivity of the single particle probe

Considering that the copper ion solution is added dropwise and assuming that the copper ions are evenly distributed in the solution, we suppose that the number of copper ions accumulated on a single particle is basically the same for each droplet. With this assumption, the number of Cu^{2+} ions detected by the single particle probe can be considered equally increase with increase of the droplet number, which is equivalent to the increase of the Cu^{2+} concentration by one droplet.

Since the luminescence intensity of the single-particle probe can also be influenced by water solvent, one need to deduct the luminescence emission contribution resulted by water solvent during the Cu^{2+} ion detection. Based on this consideration, experimental data obtained from the system with pure water solvent and Cu^{2+} ion water solution were plotted separately in the Fig. 5(a). After the contribution of water removed, the degree of luminescence quenching on the probe was plotted and fitted in Fig. 5(b). It shows that the single-particle fluorescent probe has a linear detection in the range of 20–60 nM, and the

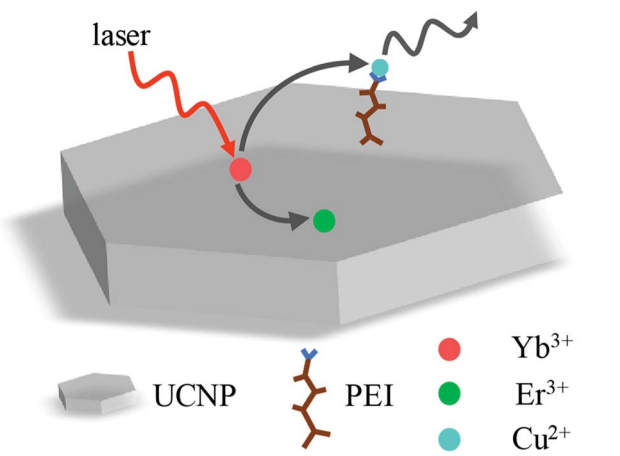

Fig. 3 Schematic of the single particle probe for detecting the concentration of copper ion solution.

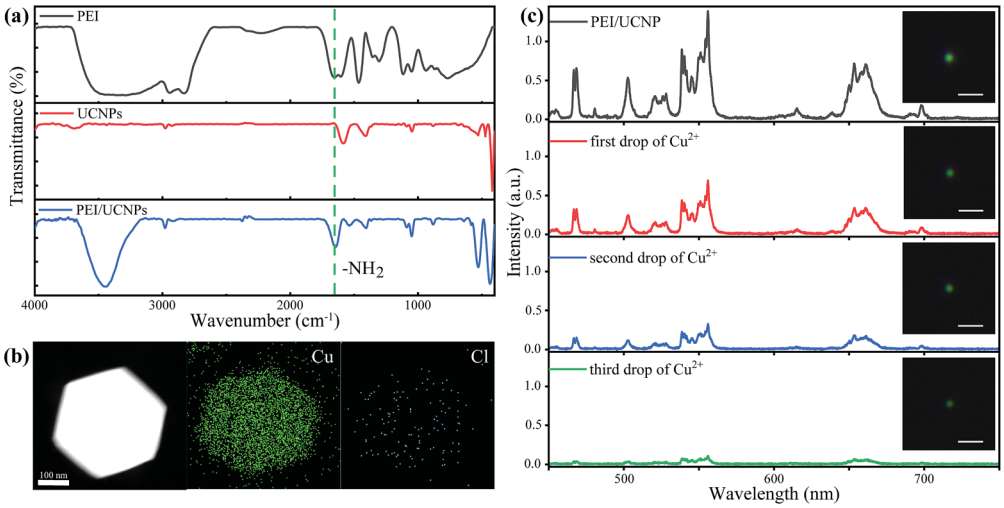

Fig. 4 (a) Fourier transform infrared spectra of the PEI, bare and PEI modified $NaYF_4$:Yb^{3+}/Er^{3+}/Zn^{2+} nanoparticles, (b) the distribution of copper and chloride ions on single particle fluorescent probe after the addition of 1 μM $CuCl_2$ solution to the particle, (c) emission spectra and corresponding microscopic images of the single particle probe before and after adding copper ion solution on it, and the scale bars are 2 μm.

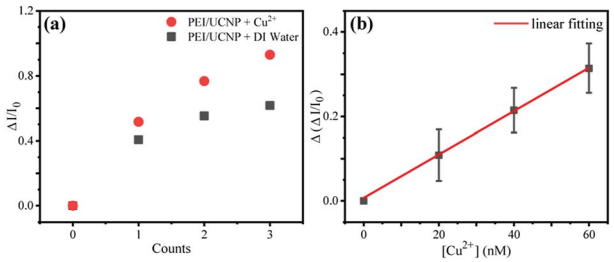

Fig. 5 (a) Luminescence quenching of the single particle fluorescent probe with 20 nM copper ion solution and water solvent, respectively (b) linear data fitting on the degree of luminescence quenching of the single particle fluorescent probe with the concentration of copper ions after taking off the solvent contribution.

detection limit is about 11 nM that is comparable to the limit detected by existing methods.[17,36,37]

In addition, the selectivity of the single particle fluorescent probe for copper ion detection was investigated. As shown in Fig. S5,† the single particle probe exhibited significantly different fluorescence quenching responses to 60 nM Cu^{2+} solution and 600 nM other ions (Fe^{3+}, Na^+, K^+, Mg^{2+}, Sn^{2+}, NH_4^+) solution. It was found that the single particle probe exhibited high selectivity towards Cu^{2+}, which can be used for copper ion detection of the tap water from the Water Supply Company. As shown in Fig. S6,† the concentration of Cu^{2+} in the tap water was between 0.3–0.6 μM according to fitting result in Fig. 5(b), which was similar to the concentration (<0.4 μM) detected by Water Supply Company.

4. Conclusions

$NaYF_4$:Yb^{3+}/Er^{3+}/Zn^{2+} nanoparticles with enhanced luminescence emission were synthesized and surface modification of the particles was performed successfully by using PEI. It was found that the PEI modified $NaYF_4$:Yb^{3+}/Er^{3+}/Zn^{2+} particle can be a good fluorescent probe for Cu^{2+} ion detection. By studying the luminescence quenching effect of the single PEI-modified $NaYF_4$:Yb^{3+}/Er^{3+}/Zn^{2+} particle, we obtained the linear detection range of 20–60 nM for the single particle probe, and the detection limit was around 11 nM. The current work offered an ion detection system with high sensitivity and selectivity, it also suggested that more single-particle fluorescent probe can be constructed for the detection of heavy metal ions and biomolecules.

Conflicts of interest

The authors declare no conflict of interest.

Acknowledgements

This work was supported by the National Natural Science Foundation of China (Grant 11574190, 11504224), the Fundamental Research Funds for Central Universities (GK201701008).

References

1 G. Y. Chen, T. Y. Ohulchanskyy, R. Kumar, H. Agren and P. N. Prasad, *ACS Nano*, 2010, **4**, 3163–3168.
2 D. J. Gargas, E. M. Chan, A. D. Ostrowski, S. Aloni, M. V. P. Altoe, E. S. Barnard, B. Sanii, J. J. Urban, D. J. Milliron, B. E. Cohen and P. J. Schuck, *Nat. Nanotechnol.*, 2014, **9**, 300–305.
3 C. S. Ma, X. X. Xu, F. Wang, Z. G. Zhou, D. M. Liu, J. B. Zhao, M. Guan, C. I. Lang and D. Y. Jin, *Nano Lett.*, 2017, **17**, 2858–2864.
4 A. D. Ostrowski, E. M. Chan, D. J. Gargas, E. M. Katz, G. Han, P. J. Schuck, D. J. Milliron and B. E. Cohen, *ACS Nano*, 2012, **6**, 2686–2692.

5 S. W. Wu, G. Han, D. J. Milliron, S. Aloni, V. Altoe, D. V. Talapin, B. E. Cohen and P. J. Schuck, *Proc. Natl. Acad. Sci. U. S. A.*, 2009, **106**, 10917–10921.
6 D. F. Peng, Q. Ju, X. Chen, R. H. Ma, B. Chen, G. X. Bai, J. H. Hao, X. S. Qiao, X. P. Fan and F. Wang, *Chem. Mater.*, 2015, **27**, 3115–3120.
7 H. Chen, P. Zhang, H. Cui, W. Qin and D. Zhao, *Nanoscale Res. Lett.*, 2017, **12**, 548.
8 S. Fischer, J. K. Swabeck and A. P. Alivisatos, *J. Am. Chem. Soc.*, 2017, **139**, 12325–12332.
9 F. Guzzetta, A. Roig and B. Julián-López, *J. Phys. Chem. Lett.*, 2017, **8**, 5730–5735.
10 F. Wang, Y. Han, C. S. Lim, Y. H. Lu, J. Wang, J. Xu, H. Y. Chen, C. Zhang, M. H. Hong and X. G. Liu, *Nature*, 2010, **463**, 1061–1065.
11 M. W. Pin, E. J. Park, S. Choi, Y. I. Kim, C. H. Jeon, T. H. Ha and Y. H. Kim, *Sci. Rep.*, 2018, **8**, 10.
12 J. J. Peng, A. Samanta, X. Zeng, S. Y. Han, L. Wang, D. D. Su, D. T. B. Loong, N. Y. Kang, S. J. Park, A. H. All, W. X. Jiang, L. Yuan, X. G. Liu and Y. T. Chang, *Angew. Chem., Int. Ed.*, 2017, **56**, 4165–4169.
13 A. Xia, Y. Y. Deng, H. Shi, J. Hu, J. Zhang, S. S. Wu, Q. Chen, X. H. Huang and J. Shen, *ACS Appl. Mater. Interfaces*, 2014, **6**, 18329–18336.
14 S. H. Nam, Y. M. Bae, Y. I. Park, J. H. Kim, H. M. Kim, J. S. Choi, K. T. Lee, T. Hyeon and Y. D. Suh, *Angew. Chem., Int. Ed.*, 2011, **50**, 6093–6097.
15 P. Hu, X. F. Wu, S. G. Hu, Z. H. Chen, H. Y. Yan, Z. F. Xi, Y. Yu, G. T. Dai and Y. X. Liu, *Photochem. Photobiol. Sci.*, 2016, **15**, 260–265.
16 Y. D. Han, H. Y. Li, Y. B. Wang, Y. Pan, L. Huang, F. Song and W. Huang, *Sci. Rep.*, 2017, **7**, 1320.
17 F. Wang, C. Zhang, Q. Xue, H. Li and Y. Xian, *Biosens. Bioelectron.*, 2017, **95**, 21–26.
18 C. X. Li, J. L. Liu, S. Alonso, F. Y. Li and Y. Zhang, *Nanoscale*, 2012, **4**, 6065–6071.
19 Z. W. Cui, W. B. Bu, W. P. Fan, J. W. Zhang, D. L. Ni, Y. Y. Liu, J. Wang, J. N. Liu, Z. W. Yao and J. L. Shi, *Biomaterials*, 2016, **104**, 158–167.
20 Y. Choi, Y. Park, T. Kang and L. P. Lee, *Nat. Nanotechnol.*, 2009, **4**, 742–746.
21 Y. Xue, C. Ding, Y. Rong, Q. Ma, C. Pan, E. Wu, B. Wu and H. Zeng, *Small*, 2017, **13**, 1701155.
22 Y. Li, X. Liu, X. Yang, H. Lei, Y. Zhang and B. Li, *ACS Nano*, 2017, **11**, 10672–10680.
23 J. Zuo, Q. Q. Li, B. Xue, C. X. Li, Y. L. Chang, Y. L. Zhang, X. M. Liu, L. P. Tu, H. Zhang and X. G. Kong, *Nanoscale*, 2017, **9**, 7941–7946.
24 S. Fischer, N. D. Bronstein, J. K. Swabeck, E. M. Chan and A. P. Alivisatos, *Nano Lett.*, 2016, **16**, 7241–7247.
25 A. Dubey, A. K. Soni, A. Kumari, R. Dey and V. K. Rai, *J. Alloys Compd.*, 2017, **693**, 194–200.
26 B. Zhou, B. Xu, H. M. He, Z. J. Gu, B. Tang, Y. Ma and T. Y. Zhai, *Nanoscale*, 2018, **10**, 2834–2840.
27 M. Ding, Y. Ni, Y. Song, X. Liu, T. Cui, D. Chen, Z. Ji, F. Xu, C. Lu and Z. Xu, *J. Alloys Compd.*, 2015, **623**, 42–48.
28 R. Dey, A. Kumari, A. K. Soni and V. K. Rai, *Sens. Actuators, B*, 2015, **210**, 581–588.
29 T. Cong, Y. D. Ding, J. P. Liu, H. Y. Zhao and X. Hong, *Mater. Lett.*, 2016, **165**, 59–62.
30 Z. H. Li, H. Yuan, W. Yuan, Q. Q. Su and F. Y. Li, *Coord. Chem. Rev.*, 2018, **354**, 155–168.
31 M. Y. Hossan, A. Hor, Q. Luu, S. J. Smith, P. S. May and M. T. Berry, *J. Phys. Chem. C*, 2017, **121**, 16592–16606.
32 A. Pliss, T. Y. Ohulchanskyy, G. Chen, J. Damasco, C. E. Bass and P. N. Prasad, *ACS Photonics*, 2017, **4**, 806–814.
33 Q. Y. Han, C. Y. Zhang, C. Wang, Z. J. Wang, C. X. Li, W. Gao, J. Dong, E. J. He, Z. L. Zhang and H. R. Zheng, *Sci. Rep.*, 2017, **7**, 5371.
34 Y. Kuang, J. T. Xu, C. Wang, C. Q. Wang, H. Shao, D. Yang, S. L. Gai, F. He and P. P. Yang, *CrystEngComm*, 2018, **20**, 2663–2668.
35 P. Du, E. J. Kim and J. S. Yu, *Curr. Appl. Phys.*, 2018, **18**, 310–316.
36 H. Shao, D. Xu, Y. Ding, X. Hong and Y. Liu, *Microchim. Acta*, 2018, **185**, 211.
37 Q. Yan, Z.-H. Chen, S.-F. Xue, X.-Y. Han, Z.-Y. Lin, S. Zhang, G. Shi and M. Zhang, *Sens. Actuators, B*, 2018, **268**, 108–114.